NASA/TM—20230006534

TESS Data Release Notes:
Sector 57, DR82

Michael M. Fausnaugh, Christopher J. Burke
Kavli Institute for Astrophysics and Space Science, Massachusetts Institute of Technology,
Cambridge, Massachusetts

Douglas A. Caldwell
SETI Institute, Mountain View, California

Jon M. Jenkins
NASA Ames Research Center, Moffett Field, California

Joseph D. Twicken
SETI Institute, Mountain View, California

Roland Vanderspek
Kavli Institute for Astrophysics and Space Science, Massachusetts Institute of Technology,
Cambridge, Massachusetts

John P. Doty
Noqsi Aerospace Ltd, Billerica, Massachusetts

Eric B. Ting
NASA Ames Research Center, Moffett Field, California

Joel S. Villasenor
Kavli Institute for Astrophysics and Space Science, Massachusetts Institute of Technology,
Cambridge, Massachusetts

December 02, 2022

NASA STI Program ... in Profile

Since its founding, NASA has been dedicated to the advancement of aeronautics and space science. The NASA scientific and technical information (STI) program plays a key part in helping NASA maintain this important role.

The NASA STI program operates under the auspices of the Agency Chief Information Officer. It collects, organizes, provides for archiving, and disseminates NASA's STI. The NASA STI program provides access to the NTRS Registered and its public interface, the NASA Technical Reports Server, thus providing one of the largest collections of aeronautical and space science STI in the world. Results are published in both non-NASA channels and by NASA in the NASA STI Report Series, which includes the following report types:

- TECHNICAL PUBLICATION. Reports of completed research or a major significant phase of research that present the results of NASA Programs and include extensive data or theoretical analysis. Includes compilations of significant scientific and technical data and information deemed to be of continuing reference value. NASA counterpart of peer-reviewed formal professional papers but has less stringent limitations on manuscript length and extent of graphic presentations.

- TECHNICAL MEMORANDUM.
  Scientific and technical findings that are preliminary or of specialized interest, e.g., quick release reports, working papers, and bibliographies that contain minimal annotation. Does not contain extensive analysis.

- CONTRACTOR REPORT. Scientific and technical findings by NASA-sponsored contractors and grantees.

- CONFERENCE PUBLICATION.
  Collected papers from scientific and technical conferences, symposia, seminars, or other meetings sponsored or co-sponsored by NASA.

- SPECIAL PUBLICATION.
  Scientific, technical, or historical information from NASA programs, projects, and missions, often concerned with subjects having substantial public interest.

- TECHNICAL TRANSLATION.
  English-language translations of foreign scientific and technical material pertinent to NASA's mission.

Specialized services also include organizing and publishing research results, distributing specialized research announcements and feeds, providing information desk and personal search support, and enabling data exchange services.

For more information about the NASA STI program, see the following:

- Access the NASA STI program home page at http://www.sti.nasa.gov

- E-mail your question to help@sti.nasa.gov

- Phone the NASA STI Information Desk at 757-864-9658

- Write to:
  NASA STI Information Desk
  Mail Stop 148
  NASA Langley Research Center
  Hampton, VA 23681-2199
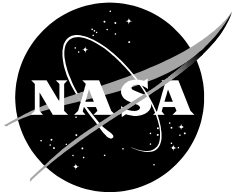
TESS Data Release Notes:
Sector 57, DR82

Michael M. Fausnaugh, Christopher J. Burke
Kavli Institute for Astrophysics and Space Science, Massachusetts Institute of Technology, Cambridge, Massachusetts

Douglas A. Caldwell
SETI Institute, Mountain View, California

Jon M. Jenkins
NASA Ames Research Center, Moffett Field, California

Jeffrey C. Smith, Joseph D. Twicken
SETI Institute, Mountain View, California

Roland Vanderspek
Kavli Institute for Astrophysics and Space Science, Massachusetts Institute of Technology, Cambridge, Massachusetts

John P. Doty
Noqsi Aerospace Ltd, Billerica, Massachusetts

Eric B. Ting
NASA Ames Research Center, Moffett Field, California

Joel S. Villasenor
Kavli Institute for Astrophysics and Space Science, Massachusetts Institute of Technology, Cambridge, Massachusetts

December 02, 2022

Acknowledgements

These Data Release Notes provide information on the processing and export of data from the Transiting Exoplanet Survey Satellite (TESS). The data products included in this data release are full frame images (FFIs), target pixel files, light curve files, collateral pixel files, cotrending basis vectors (CBVs), and Data Validation (DV) reports, time series, and associated xml files.

These data products were generated by the TESS Science Processing Operations Center (SPOC, Jenkins et al., 2016) at NASA Ames Research Center from data collected by the TESS instrument, which is managed by the TESS Payload Operations Center (POC) at Massachusetts Institute of Technology (MIT). The format and content of these data products are documented in the Science Data Products Description Document (SDPDD)[1]. The SPOC science algorithms are based heavily on those of the Kepler Mission science pipeline, and are described in the Kepler Data Processing Handbook (Jenkins, 2020).[2] The Data Validation algorithms are documented in Twicken et al. (2018) and Li et al. (2019). The TESS Instrument Handbook (Vanderspek et al., 2018) contains more information about the TESS instrument design, detector layout, data properties, and mission operations.

The TESS Mission is funded by NASA's Science Mission Directorate.

This report is available in electronic form at
https://archive.stsci.edu/tess/

---

[1]https://archive.stsci.edu/missions/tess/doc/EXP-TESS-ARC-ICD-TM-0014-Rev-F.pdf
[2]https://archive.stsci.edu/kepler/manuals/KSCI-19081-003-KDPH.pdf

1 Observations

TESS Sector 57 observations include physical orbits 121 and 122 of the spacecraft around the Earth. Data collection was paused for a total of 0.63 days to download data. Data were downloaded approximately every seven days, once near apogee of each orbit and once near perigee.

At TJD 2863.28, the spacecraft entered into safe mode, resulting in instrument turn-off until TJD 2866.41. There are no FFIs, target pixel file data, or light curve data during this time. During these times (as well as when the spacecraft is transmitting data to ground systems) the data and timestamps in target-pixel files and light curve files are set to NULL.

In total, there are 25.00 days of science data collected in Sector 57.

Table 1: Sector 57 Observation times

	UTC	TJD^a	Cadence #
Orbit 121a start	2022-09-30 20:20:44	2853.34923	1170644
Orbit 121a end	2022-10-08 01:46:44	2860.57561	1175847
Orbit 121b start	2022-10-08 06:50:44	2860.78672	1175999
Safe Mode Start	2022-10-10 18:42:28	2863.28030	1177794
Safe Mode End	2022-10-13 21:48:24	2866.40941	1180047
Orbit 121b end	2022-10-14 17:52:44	2867.24644	1180650
Orbit 122a start	2022-10-14 22:54:44	2867.45616	1180801
Orbit 122a end	2022-10-22 02:32:43	2874.60755	1185950
Orbit 122b start	2022-10-22 07:34:43	2874.81727	1186101
Orbit 122b end	2022-10-29 14:42:43	2882.11449	1191355

^{a} TJD = TESS JD = JD - 2,457,000.0

^{b}The horizontal black lines mark gaps in the light curves for data downlink.

The spacecraft was pointing at RA (J2000): 344.2275°; Dec (J2000): 56.4121°; Roll: 44.0100°. See the TESS project Sector 57 observation page[3] for the coordinates of the spacecraft pointing and center field-of-view of each camera. Fields-of-view for each camera can be found at the TESS Guest Investigator Office observations status page.[4] The detailed target list for both 2-minute and 20-second data, as well as the Guest Investigator target lists, can be found at the Sector 57 observation page and the observations status page.

1.1 Notes on Individual Targets

There are no issues with missing light curves in the 20-second data products. There were 2309 targets chosen for 20-second cadence observations, including 400 PPA stars. TIC 441804565, 341873045, and 1551711135 are blended with comparably bright stars—the contaminating flux for these objects is very large, and the resulting photometry is expected to be unreliable.

For the 2-minute cadence data, 13000 targets were selected. Two bright stars (Tmag $\lesssim$ 1.8) with large pixel stamps were not processed in the photometric pipeline. The target pixel

---

[3]https://tess.mit.edu/observations/sector-57

[4]https://heasarc.gsfc.nasa.gov/docs/tess/sector.html

files with original and calibrated pixel data are provided, but no light curves were produced. Note that the TPF files do not include a background correction for stars without light curves. The affected TIC IDs are 174500619 and 260614141.

Five target stars (502687433, 441804565, 341873045, 2022482049, 1551711135) are blended with comparably bright stars—the contaminating flux for these objects is very large, and the resulting photometry is expected to be unreliable.
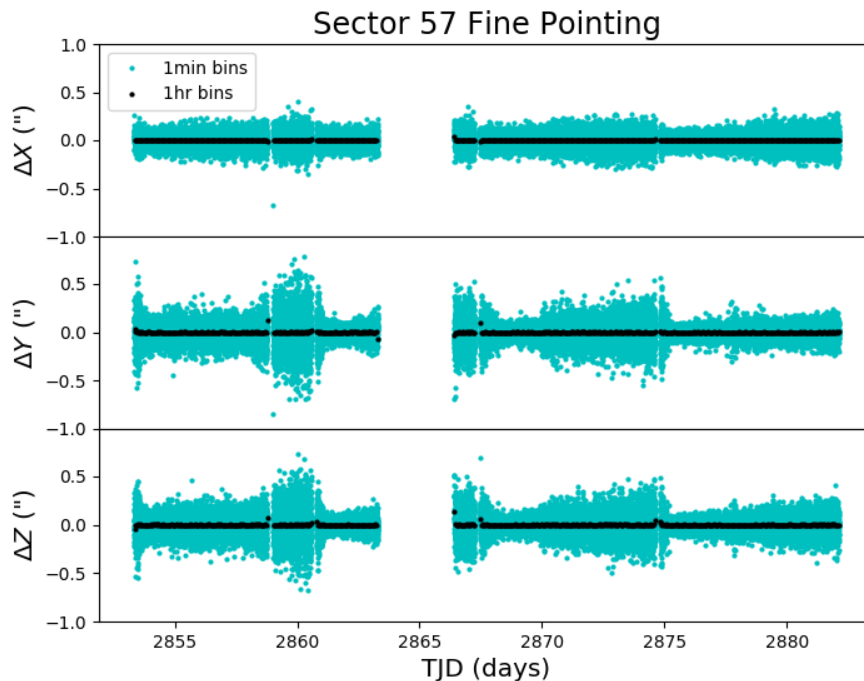
Figure 1: The delta-quaternions from each camera have been converted to spacecraft frame, binned to 1 minute and 1 hour. Long-term trends (such as those caused by differential velocity aberration) have also been removed. The ΔX/ΔY directions represent offsets along the detectors' rows/columns, while the ΔZ direction represents spacecraft roll.

1.2 Spacecraft Pointing and Momentum dumps

The pointing in Sector 57 was set at +54 degrees in ecliptic latitude so, so that Camera 4 was pointed at the North Ecliptic Pole. Camera 1 and Camera 4 alone were used for guiding in both orbit 121 and 122, except for the second half of orbit 121 in which Camera 4 alone was used for guiding. One momentum dump was performed in each orbit, at the end of each data downlink just before data collection resumed. Figure 1 summarizes the pointing performance over the course of the sector based on Fine Pointing telemetry.

1.3 Scattered Light

Figure 2 shows the median value of the background estimate for all targets on a given CCD as a function of time. Figure 3 shows the angle between each camera's boresight and the

Earth or Moon—this figure can be used to identify periods affected by scattered light and the relative contributions of the Earth and Moon to the image backgrounds.

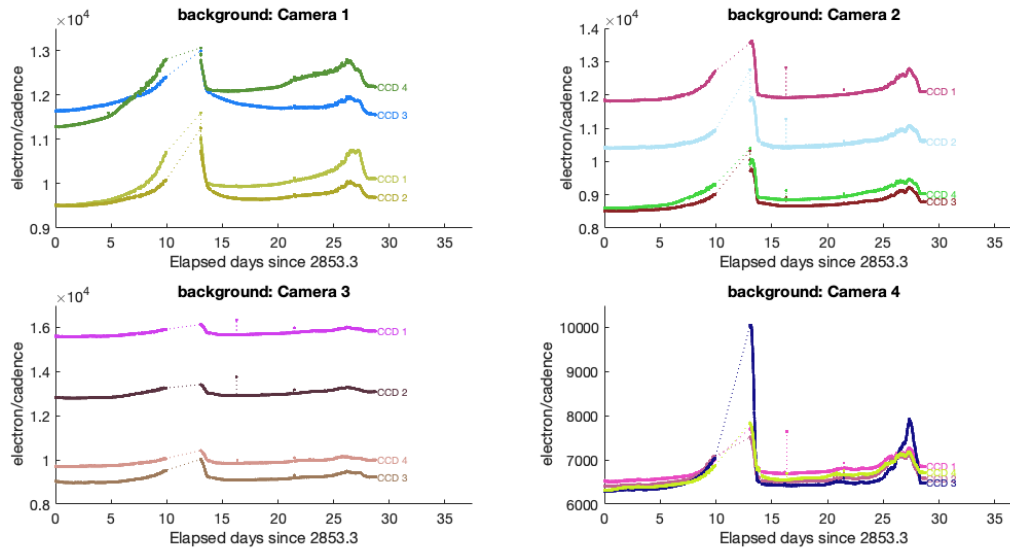In Sector 57, the Moon introduces scattered light signals towards the second half of orbit 1.

Figure 2: Median background flux across all targets on a given CCD in each camera. The changes are caused by variations in the orientation and distance of the Earth and Moon.

2   Data Anomaly Flags

See the SDPDD (§9) for a list of data quality flags and the associated binary values used for TESS data, and the TESS Instrument Handbook for a more detailed description of each flag.

The following flags were not used in Sector 57: bits 1 and 9 (Attitude Tweak and Discontinuity).

Cadences marked with bits 2, 3, 4, 6, and 12 (Safe Mode, Coarse Point, Earth Point, Reaction Wheel Desaturation Event, and Straylight) were marked based on spacecraft telemetry. Cadences marked with bits 2 and 4 (Safe Mode and Earth Point) have timestamps and data marked with NULL in the target-pixel files and light curve files.

Cadences marked with bit 5 and 10 (Argabrightening Events and Impulsive Outlier) were identified by the SPOC pipeline. Bit 5 marks a sudden change in the background measurements. In practice, bit 5 flags are caused by rapidly changing glints and unstable pointing at times near momentum dumps. Bit 10 marks an outlier identified by PDC and omitted from the cotrending procedure.

The 20-second data mode includes cadences marked with bit 7 and 11 (Cosmic Ray in Optimal Aperture and Cosmic Ray in Collateral Pixel). These flags indicate cadences affected by cosmic rays that are removed by the pipeline, and can be found in both the TPF and LC files. The data provided in the archive products are corrected for cosmic rays, and a
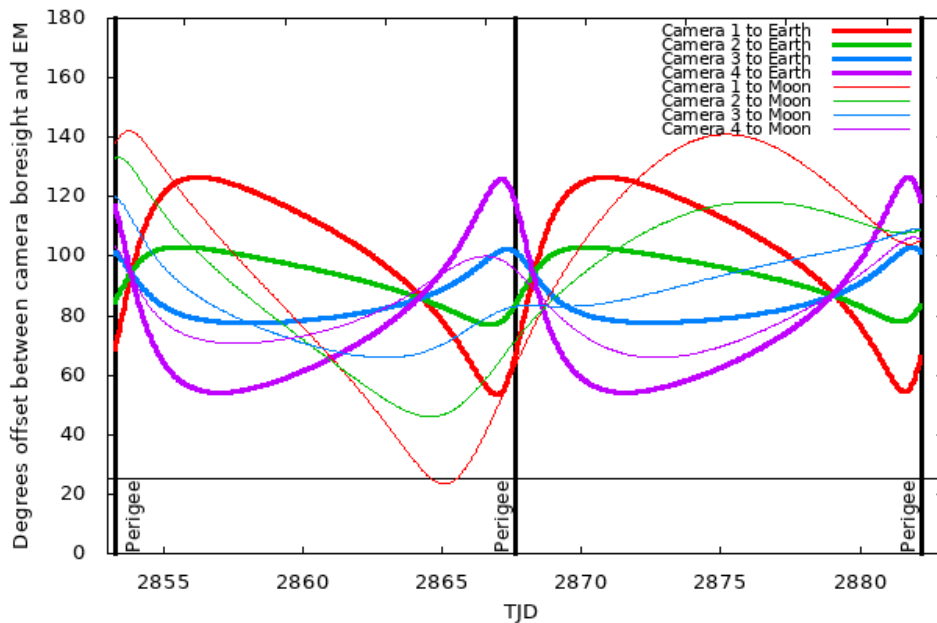
3

Figure 3: Angle between the four camera boresights and the Earth/Moon as a function of time. When the Earth is within $\sim 25°$ of a camera's boresight, transiting planet searches may be compromised by high levels of scattered light. At larger angles, up to $\sim 35°$, scattered light patterns and complicated structures may be visible. At yet larger angles, low level patchy features may be visible. Scattered light from the Moon is generally only noticeable below $\sim 35°$. This figure can be used to identify periods affected by scattered light and the relative contributions of the Earth and Moon to the background. However, the background intensity and locations of scattered light features depend on additional factors, such as the Earth/Moon azimuth and distance from the spacecraft.

FITS table extension in the TPF and Collateral Pixel File details the cosmic rays identified and removed by the pipeline at the pixel level.

Cadences marked with bit 8 (Manual Exclude) are ignored by PDC, TPS, and DV for cotrending and transit searches. In Sector 57, these cadences were identified using spacecraft telemetry from the fine pointing system. All cadences with pointing excursions >7 arcsec (0.3 pixel) were flagged for manual exclude. Figure 4 shows an assessment of the performance of the cotrending based on the final set of manual excludes.

The predicted stray light flag (bit 12, value 2048) is marked in the FFIs and flags times when the Earth/Moon are near the camera FOVs and may interfere with guiding or saturate the detectors. We strongly recommend that users inspect the FFI data before removing images marked with bit 12, because this bit is set based on predictions from mission planning and is known to be conservative with respect to the quality of data usable for analysis.

The predicted stray light flag (bit 12) is disabled for the 2-minute and 20-second data products. The scattered light exclude flag (bit 13, value 4096) identifies cadences at which individual targets are affected by scattered light
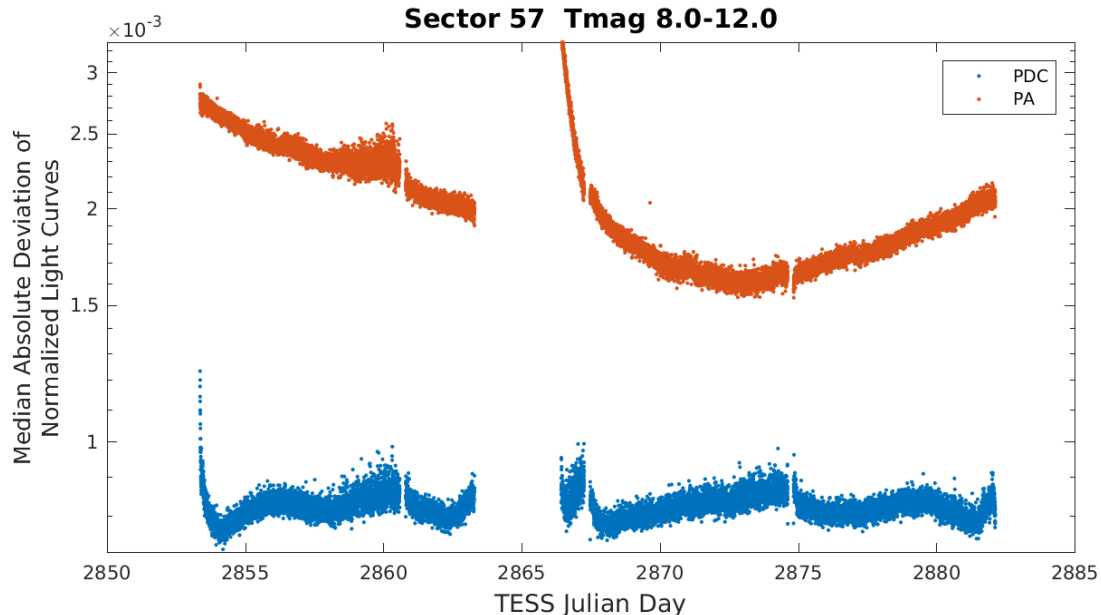
4

Figure 4: Median absolute deviation (MAD) for the two-minute cadence data from Sector 57, showing the performance of the cotrending after identifying Manual Exclude data quality flags. The MAD is calculated in each cadence across stars with flux variations less than 1% for both the PA (red) and PDC (blue) light curves, where each light curve is normalized by its median flux value. The scatter in the PA light curves is much higher than that for the PDC light curves, and the outliers in the PA light curves are largely absent from the PDC light curves due to the use of the anomaly flags.

If the Earth/Moon interference is strong enough to saturate the detector, all targets on a CCD slice will be affected and the data are unusable. Cadences with bad calibrations due to saturation are now explicitly marked with bit 15 (value 16384, "Bad Calibration Exclude"). For some cadences, the majority of targets on a CCD may be flagged for scattered light and not enough valid data remains to derive cotrending basis vectors in PDC. No systematic error correction can be applied at these times. This situation is identified by bit 16 (value 32768, "Insufficient Targets for Error Correction Exclude").

FFIs were only marked with bits 3, 6, 8, 12, and 15 (Coarse Point, Reaction Wheel Desaturation Events, Manual Exclude, Straylight, and Bad Calibration Exclude). Only one FFI is affected by each momentum dump. There are no WCS coordinates for FFIs that coincide with momentum dumps.

3 Anomalous Effects

Smear Correction Issues

The following columns were impacted by bright stars in the science frame, and/or upper buffer rows, and/or lower science frame rows, which bleed into the upper serial register resulting in an overestimated smear correction.

- Camera 1, CCD 1, Column 1649 - Star BD+26 154

- Camera 1, CCD 2, Column 1417 - Star HD 784

- Camera 1, CCD 3, Column 795 - Star HD 1048

- Camera 1, CCD 3, Column 902 - Star BD+21 19

- Camera 1, CCD 3, Column 1091 - Star BD+22 49

- Camera 1, CCD 3, Column 1433 - Star BD+23 63

- Camera 1, CCD 4, Column 1710 - Star HD 8815

- Camera 2, CCD 2, Column 241 - Star Lambda Andromedae

- Camera 2, CCD 4, Column 274 - Star HD 224100

- Camera 4, CCD 2, Column 134 - Star BD+66 1051

- Camera 4, CCD 2, Column 588 - Star HD 160832

- Camera 4, CCD 2, Column 1353 - Star TYC 4424-81-1

- Camera 4, CCD 2, Column 1562 - Star HD 154928

- Camera 4, CCD 3, Column 103 - Star HD 134807

- Camera 4, CCD 3, Column 1240 - Star HD 15806

- Camera 4, CCD 3, Column 1655 - Star BD+67 1023

- Camera 4, CCD 3, Column 1763 - Star HD 160862

- Camera 4, CCD 3, Column 2046 - Star TYC 4208-736-1

- Camera 4, CCD 4, Column 486 - Star BD+62 1588

- Camera 4, CCD 4, Column 521 - Star BD+62 1589

- Camera 4, CCD 4, Column 1109 - Star HD 166579

4 Pipeline Performance and Results

4.1 Light Curves and Photometric Precision

Figure 5 gives the PDC goodness metrics for the two-minute cadence data, with residual correlation goodness and introduced noise goodness shown on a scale between 0 (bad) and 1 (good). The performance of PDC is very good and generally uniform over most of the field of view. Figure 6 shows the achieved Combined Differential Photometric Precision (CDPP) at 1-hour timescales for all two-minute targets.
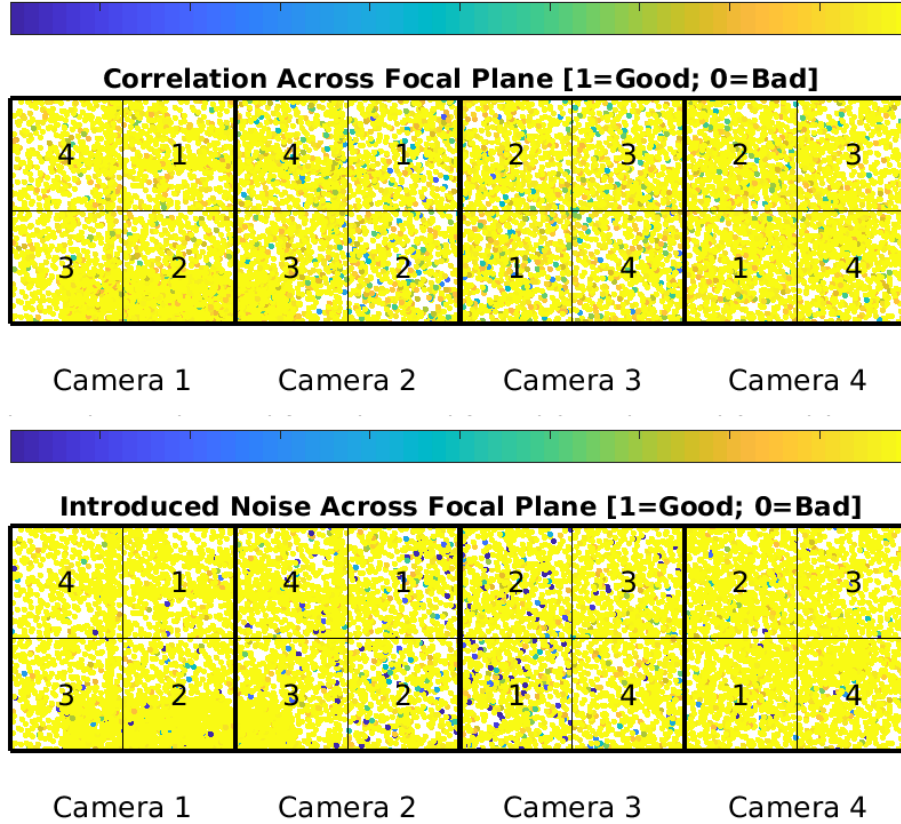
Figure 5: PDC residual correlation goodness metric (top panel) and PDC introduced noise goodness metric (bottom panel) for the two-minute cadence data. The metric values are shown on a focal plane map indicating the camera and CCD location of each target. The correlation goodness metric is calibrated such that a value greater than 0.8 means there is less than 10% mean absolute correlation between the target under study and all other targets on the CCD. The introduced noise metric is calibrated such that a value greater than 0.8 means the power in broad-band introduced noise is below the level of uncertainties in the flux values.

4.2   Transit Search and Data Validation

In Sector 57, the two-minute light curves of 12998 targets were subjected to the transit search in TPS. Of these, Threshold Crossing Events (TCEs) at the $7.1\,\sigma$ level were generated for 1161 targets.

We employed an iterative method when conducting the Sector 57 transit search. The top panel of Figure 7 shows the number of TCEs at a given cadence that exhibit a transit signal from an initial run of TPS. The 3-σ peaks were used to define de-emphasis weights for a second run of TPS, the results of which are shown in the bottom panel of Figure 7. The final set of TCEs and the results reported here are based on the second run of TPS. The values of the adopted de-emphasis weights are provided in the DV timeseries data products for targets with TCEs.

The top panel of Figure 8 shows the distribution of orbital periods for the final set of TCEs found in Sector 57. The bimodal nature of the period distribution is due to a large
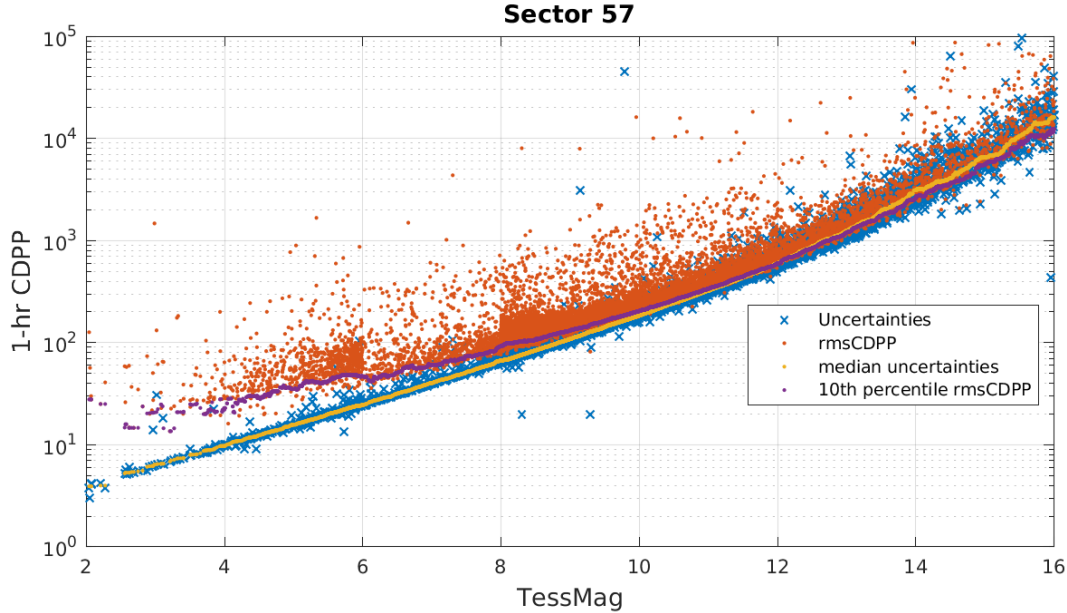
Figure 6: 1-hour CDPP. The red points are the RMS CDPP measurements for the 12998 light curves from Sector 57 plotted as a function of TESS magnitude. The blue x's are the uncertainties, scaled to 1-hour timescale. The purple curve is a moving 10th percentile of the RMS CDPP measurements, and the gold curve is a moving median of the 1-hr uncertainties.

number of two-transit detections with periods ranging from 8 to 20 days, many of which are likely false positives. Two-transit TCEs can be identified with the NTRANS keyword in the headers of the dv-timeseries FITS files. The vertical histogram in the right panel of Figure 8 shows the distribution of transit depths derived from limb-darkened transiting planet model fits for TCEs. The model transit depths range down to the order of 100 ppm, but the bulk of the transit depths are considerably larger.

A search for additional TCEs in potential multiple planet systems was conducted in DV through calls to TPS. A total of 1694 TCEs were ultimately identified in the SPOC pipeline on 1161 unique target stars. Table 2 provides a breakdown of the number of TCEs by target. Note that targets with large numbers of TCEs are likely to include false positives.

Table 2: Sector 57 TCE Numbers

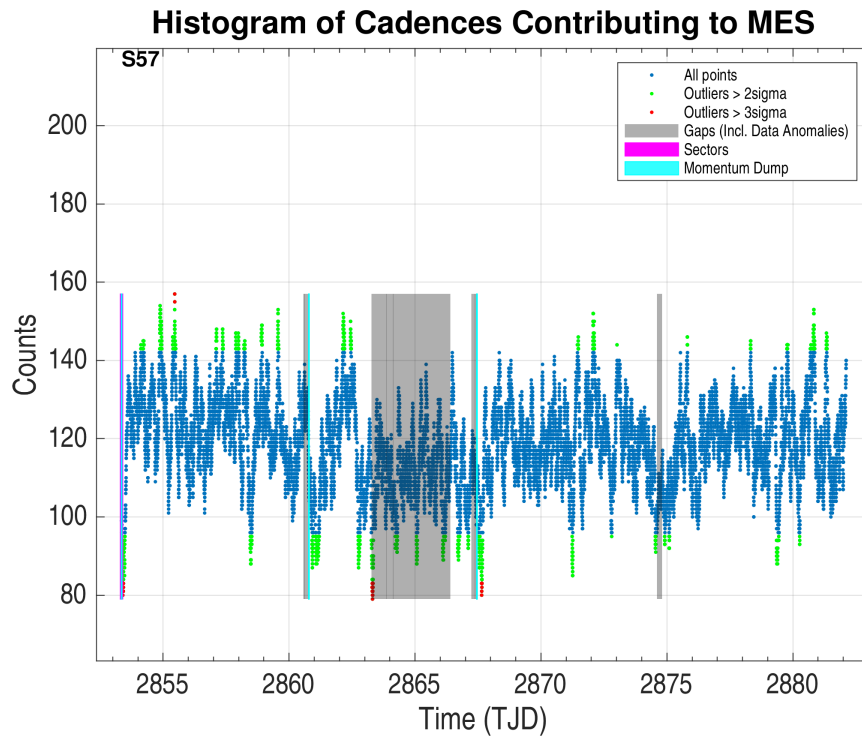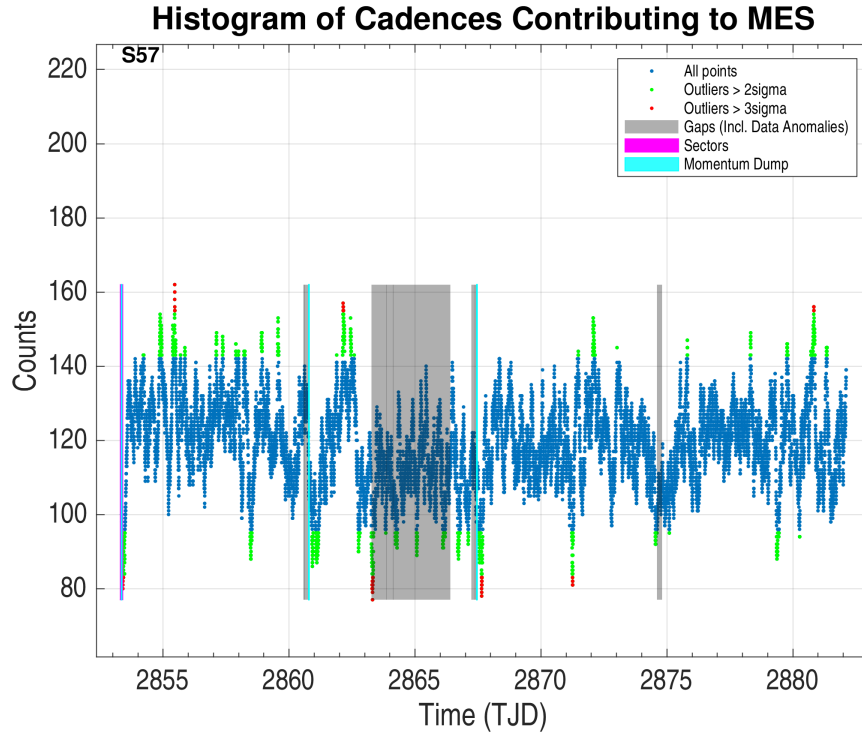| Number of TCEs	Number of Targets	Total TCEs
1	748	748
2	321	642
3	68	204
4	21	84
5	2	10
6	1	6
–	1161	1694

8

Figure 7: Top panel: Number of TCEs at a given cadence exhibiting a transit signal, based on an initial run of TPS. Any isolated peaks are caused by single events that result in spurious TCEs. These peaks were used to define de-emphasis weights that suppress problematic epochs for the transit detection statistics in a second iteration of TPS. Bottom panel: Results from the second run of TPS.
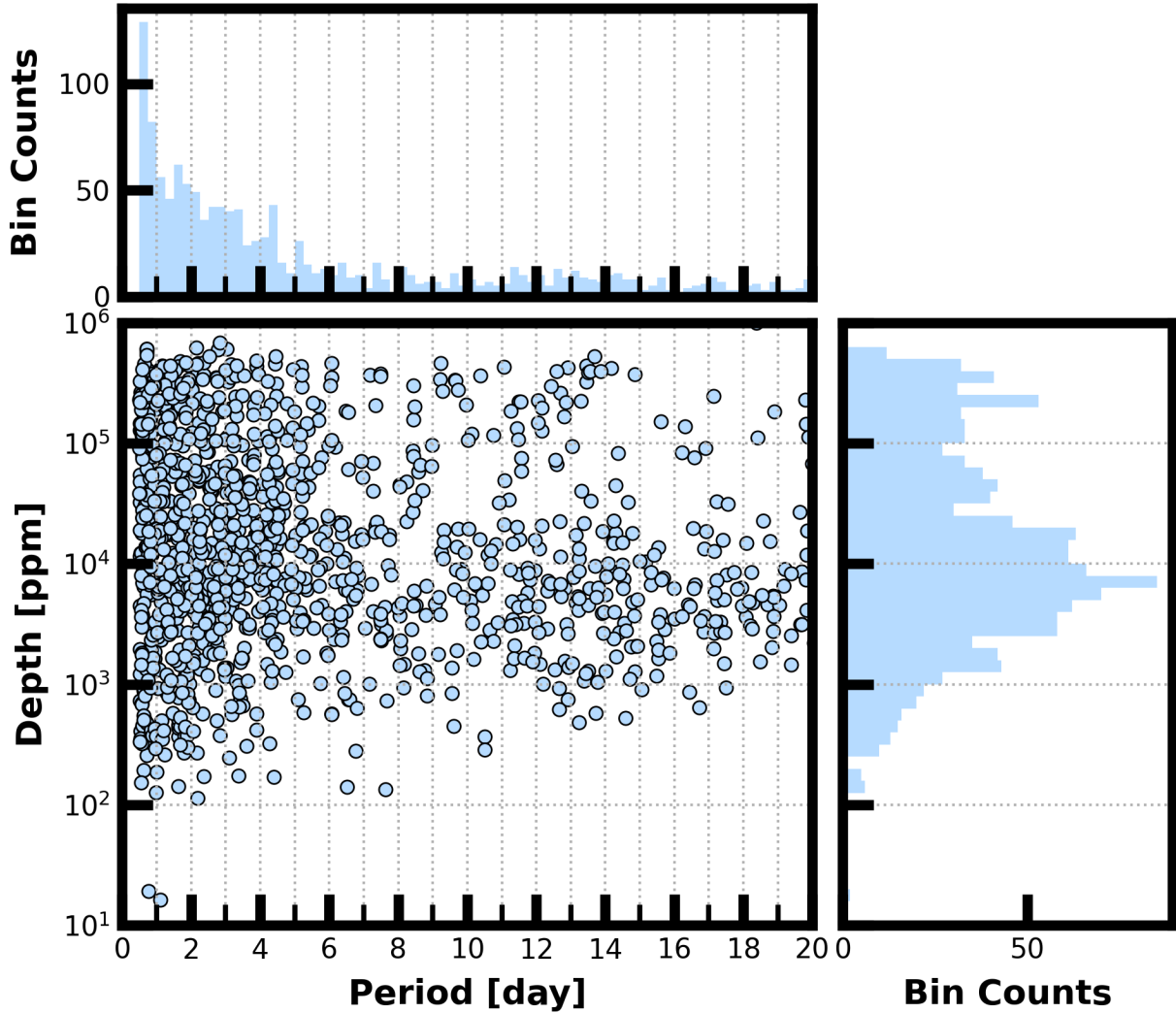
Figure 8: Lower Left Panel: Transit depth as a function of orbital period for the 1694 TCEs identified for the Sector 57 search. For enhanced visibility of long period detections, TCEs with orbital period <0.5 days are not shown. Reported depth comes from the DV limb-darkened transit fit depth when available, and the DV trapezoid model fit depth when not available. Top Panel: Orbital period distribution of the TCEs shown in the lower left panel. Right Panel: Transit depth distribution for the TCEs shown in the lower left panel.

References

Jenkins, J. M. 2020, Kepler Data Processing Handbook: Overview of the Science Operations Center, Tech. rep., NASA Ames Research Center

Jenkins, J. M., Twicken, J. D., McCauliff, S., et al. 2016, in Proc. SPIE, Vol. 9913, Software and Cyberinfrastructure for Astronomy IV, 99133E, doi: 10.1117/12.2233418

Li, J., Tenenbaum, P., Twicken, J. D., et al. 2019, *PASP*, 131, 024506, doi: 10.1088/1538-3873/aaf44d

Twicken, J. D., Catanzarite, J. H., Clarke, B. D., et al. 2018, *PASP*, 130, 064502, doi: 10.1088/1538-3873/aab694

Vanderspek, R., Doty, J., Fausnaugh, M., et al. 2018, TESS Instrument Handbook, Tech. rep., Kavli Institute for Astrophysics and Space Science, Massachusetts Institute of Technology

Acronyms and Abbreviation List

BTJD Barycentric-corrected TESS Julian Date

CAL Calibration Pipeline Module

CBV Cotrending Basis Vector

CCD Charge Coupled Device

CDPP Combined Differential Photometric Precision

COA Compute Optimal Aperture Pipeline Module

CSCI Computer Software Configuration Item

CTE Charge Transfer Efficiency

Dec Declination

DR Data Release

DV Data Validation Pipeline Module

DVA Differential Velocity Aberration

FFI Full Frame Image

FIN FFI Index Number

FITS Flexible Image Transport System

FOV Field of View

FPG Focal Plane Geometry model

KDPH Kepler Data Processing Handbook

KIH Kepler Instrument Handbook

KOI Kepler Object of Interest

MAD Median Absolute Deviation

MAP Maximum A Posteriori

MAST Mikulski Archive for Space Telescopes

MES Multiple Event Statistic

NAS NASA Advanced Supercomputing Division

PA Photometric Analysis Pipeline Module

PDC Pre-Search Data Conditioning Pipeline Module

PDC-MAP Pre-Search Data Conditioning Maximum A Posteriori algorithm

PDC-msMAP Pre-Search Data Conditioning Multiscale Maximum A Posteriori algorithm

PDF Portable Document Format

POC Payload Operations Center

POU Propagation of Uncertainties

PPA Photometer Performance Assessment

ppm Parts-per-million

PRF Pixel Response Function

RA Right Ascension

RMS Root Mean Square

SAP Simple Aperture Photometry

SDPDD Science Data Products Description Document

SNR Signal-to-Noise Ratio

SPOC Science Processing Operations Center

SVD Singular Value Decomposition

TCE Threshold Crossing Event

TESS Transiting Exoplanet Survey Satellite

TIC TESS Input Catalog

TIH TESS Instrument Handbook

TJD TESS Julian Date

TOI TESS Object of Interest

TPS Transiting Planet Search Pipeline Module

UTC Coordinated Universal Time

WCS World Coordinate System

XML Extensible Markup Language